symmetry

MDPI

Article

Crystal Structure of Chiral Drug Prenalterol and Its Precursor Prone to Spontaneous Resolution

Alexander A. Bredikhin *, Robert R. Fayzullin and Zemfira A. Bredikhina

Arbuzov Institute of Organic and Physical Chemistry, FRC Kazan Scientific Center of RAS, Arbuzov St. 8, Kazan 420088, Russia; fayzullin@iopc.ru (R.R.F.); zemfira@iopc.ru (Z.A.B.)
* Correspondence: baa@iopc.ru

Abstract: Due to the chiral uniformity of proteins and carbohydrates, the basic building blocks of living matter, the mirror symmetry characteristics of drugs are of exceptional importance for medicinal chemistry. In this work, we present a new synthesis of the mono-enantiomeric chiral drug prenalterol **1** based on the symmetry-breaking phenomenon, namely, the spontaneous resolution of 4-hydroxyphenyl glycerol ether **2**. The single crystal X-ray diffraction method was used to investigate both *rac*- and (*S*)-**1** as well as (*R*)-**2**. A feature of the main crystal-forming supramolecular motif (SMM) for diol **2** is the participation of three different molecules representing different types of hydroxyl groups in the formation of its repeating unit. The type of prenalterol SMM, as in the case of the related drugs propranolol **3** and pindolol **4**, appears to be a chirality driven property, and is dictated by the enantiomeric composition of the crystals. In single-enantiomeric forms, infinite one-dimensional chains are realized, organized around helical axes, while in racemates, zero-dimensional cycles are realized, organized around inversion symmetry elements. The results obtained again demonstrate the influence of the chiral polarization of a substance not only on the general (selection of a space group), but also on particular characteristics of matter crystal organization, namely selection of a specific SMM.

Keywords: chiral drug; adrenobloker; conglomerate; racemic compound; chiral separation; crystal structure; chirality-dependent supramolecular synthons

Citation: Bredikhin, A.A.; Fayzullin, R.R.; Bredikhina, Z.A. Crystal Structure of Chiral Drug Prenalterol and Its Precursor Prone to Spontaneous Resolution. *Symmetry* **2022**, *14*, 1150. https://doi.org/10.3390/sym14061150

Academic Editor: Josef Jampilek

Received: 17 May 2022
Accepted: 31 May 2022
Published: 2 June 2022

1. Introduction

The first printed mention of the possibility of non-coincidence in the space of mirror-identical objects can be found in Immanuel Kant, who wrote in 1783 (quote from [1]), "What can be more similar in every respect and in every part more alike to my hand and to my ear, than their images in a mirror? And yet I cannot put such a hand as is seen in the glass in the place of its archetype; for if this is a right hand, that in the glass is a left one, {...} and the glove of one hand cannot be used for the other." The modern term "chirality" for this phenomenon was introduced a hundred years later, in 1893, by Lord Kelvin in his Second Robert Boyle Lecture "The Molecular Tactics of a Crystal" [2]. The history of the penetration of the ideas of mirror dissymmetry into the chemical and biological sciences has been described in detail by Joseph Gal [3,4]. Modern natural science ideas about asymmetry due to chirality are reflected in the book [5], and specific aspects related to the mysteries of the origin of life in the review [6].

Attention to the specifics of the behavior of a substance, controlled by the stereochemical features of its structure and/or composition, among practical chemists has increased many times after the publication of the U.S. Food and Drug Administration rules governing the registration of new chiral drugs for the U.S. market [7,8]. Regulatory requirements to provide test results for both enantiomers when a racemic drug is introduced to the market have significantly increased the cost of the development phase, making it very difficult for new racemic synthetic drugs to enter the market. With the continuing growth of costs for

these purposes [9], the role of the stereochemical factor in the process of developing new drugs is only increasing.

The subject of this publication is the chiral drug prenalterol **1** (Scheme 1), which, since its introduction, has been registered as an individual (*S*)-enantiomer [10].

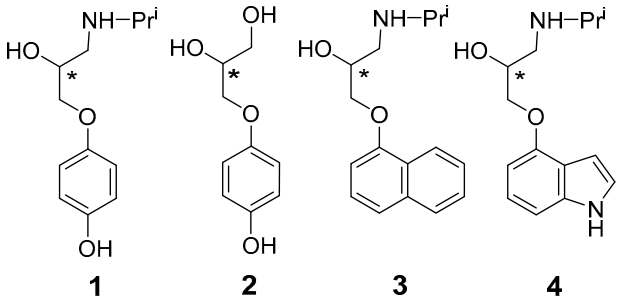

Scheme 1. Prenalterol **1**, its potential precursor 3-(4-hydroxyphenoxy)propane-1,2-diol **2**, beta-blockers propranolol **3**, and pindolol **4**. Asterisks in the diagram indicate chiral centers.

First, we propose a new method for its preparation from a synthetic precursor, namely 3-(4-hydroxyphenoxy)propane-1,2-diol **2** (Scheme 1), which is readily available in an enantiopure form due to its spontaneous resolution into enantiomers at crystallization. Secondly, we touch briefly on the crystal organization of this diol. Finally, we reveal the features of the crystal structure of racemic and enantiopure prenalterol and compare them with the available information in the literature for similar pairs of chiral drugs with similar structures and pharmacological profiles, namely propranolol **3** and pindolol **4.**

2. Materials and Methods

2.1. Instrumentation

Melting points for general purposes were determined using a Boëtius apparatus. Optical rotations were measured on a Perkin-Elmer model 341 polarimeter (PerkinElmer, Waltham, MA, USA), concentration c is given as g/100 mL. Enantiomeric purity (*ee*) was checked by HPLC analysis performed on a Shimadzu LC-20AD system controller (SHIMADZU CORPORATION, Kyoto, Japan), and a UV monitor 275 nm was used as a detector.

2.2. Materials

The synthesis of the racemic and enantiopure samples of the compounds **1** and **2** has been described in detail in our preliminary communication [11]. The single crystals of the compounds *rac*-**1-2**, (*S*)-**1,** and (*R*)-**2** were prepared by slow evaporation of solutions of the corresponding samples in appropriating solvent ((*S*)-**1**, *rac*-**1** from methanol, (*R*)-**2** from ethyl acetate, and *rac*-**2** from mixture methanol/ethyl acetate).

The characteristics of the obtained crystals agree with literature data [11] and are shown below:

(*S*)-1-(4-Hydroxyphenoxy)-3-isopropylamino-propan-2-ol, (*S*)-prenalterol, (*S*)-**1**: mp 125-127 °C, $[\alpha]_D^{20}$ –1.9 (*c* 1.0, MeOH), $[\alpha]_D^{20}$ –21.0 (*c* 1.0, 0.1N HCl); 98% *ee* (chiral HPLC analysis, Chiralcel OD-RH column; column temperature 25 °C; flow rate 0.5 mL·min^{-1}; eluent, 0.05M NH_4PF_6 aq./CH_3CN (9:1); t_R = 18.8 min (minor) and t_R = 24.6 min (major)).

rac-1-(4-Hydroxyphenoxy)-3-isopropylamino-propan-2-ol, *rac*-prenalterol, *rac*-**1**: mp 158–160 °C.

(*R*)-3-(4-Hydroxyphenoxy)propane-1,2-diol, (*R*)-**2**: mp 150–151 °C; $[\alpha]_D^{20}$ –8.2 (*c* 1.0, MeOH); 99% *ee* (chiral HPLC analysis, Chiralcel OD column; column temperature 25 °C; flow rate 1.0 mL·min^{-1}; eluent, hexane/2-propanol/TFA (7:3:0.005); t_R = 9.3 min (major) and t_R = 12.8 min (minor)).

rac-3-(4-Hydroxyphenoxy)propane-1,2-diol, *rac*-**2**: Mp 127–129 °C.

2.3. Single Crystal X-ray Diffraction

2.3.1. General Information

The X-ray diffraction data for the single crystals of *rac*- and (*S*)-**1** were collected on a Bruker D8 QUEST diffractometer with a PHOTON III area detector and an IμS DIAMOND microfocus X-ray tube using Mo *Kα* (0.71073 Å) radiation. The dataset for the single crystal of compound **2** was collected on a Rigaku XtaLab PRO instrument with a PILATUS3 R 200K hybrid pixel array detector and a MicroMax^{TM}-003 microfocus X-ray tube using Mo *Kα* radiation. The diffractometers were equipped with an Oxford Cryostream LT device or a Rigaku GN2 system for low temperature experiments. The data reduction packages APEX4 v2021.10-0 or *CrysAlisPro* 1.171.40.84a were used for data collecting and processing. Data were corrected for systematic errors and absorption. Numerical absorption correction was based on integration over a multifaceted crystal model and empirical absorption correction was based on spherical harmonics according to the point group symmetry using equivalent reflections. The structures were solved by the direct methods using SHELXT-2018/2 [12] and refined by the full-matrix least-squares on F^2 using SHELXL-2018/3 [13]. Non-hydrogen atoms were refined anisotropically. The hydrogen atoms [O–]H and [N–]H were found from Fourier difference maps and refined isotropically. The positions of the hydrogen atoms of the methyl group were found using a rotating group refinement with idealized tetrahedral angles. The other hydrogen atoms were inserted at the calculated positions and refined as riding atoms.

Deposition numbers 2167664 [(*S*)-**1**], 2167665 (*rac*-**1**), and 2167663 [(*R*)-**2**] contain the supplementary crystallographic data for this paper. These data are provided free of charge by the joint Cambridge Crystallographic Data Centre and Fachinformationszentrum Karlsruhe Access Structures service www.ccdc.cam.ac.uk/structures, accessed on 16 May 2022.

2.3.2. Crystallographic Data for (*S*)-**1**

$C_{12}H_{19}NO_3$, colorless plank (0.503 × 0.264 × 0.060 mm^3), formula weight 225.28 g mol^{-1}; orthorhombic, $P2_12_12_1$ (No. 19), a = 7.2801(3) Å, b = 9.7663(4) Å, c = 17.2342(7) Å, V = 1225.35(9) Å^3, Z = 4, Z' = 1, T = 105(2) K, d_{calc} = 1.221 g cm^{-3}, μ(Mo *Kα*) = 0.087 mm^{-1}, $F(000)$ = 488; $T_{max/min}$ = 0.9620/0.8862; 28848 reflections were collected ($2.364° \leq \theta \leq 31.758°$, index ranges: $-10 \leq h \leq 10$, $-14 \leq k \leq 14$, and $-25 \leq l \leq 25$), 4167 of which were unique, R_{int} = 0.0538, R_σ = 0.0333; completeness to θ of 31.758° 100.0%. The refinement of 159 parameters with no restraints converged to $R1$ = 0.0395 and $wR2$ = 0.0904 for 3699 reflections with $I > 2\sigma(I)$, $R1$ = 0.0486 and $wR2$ = 0.0960 for all data with goodness-of-fit S = 1.032 and residual electron density $\rho_{max/min}$ = 0.286 and −0.187 e Å^{-3}, rms 0.040; max shift/e.s.d. in the last cycle 0.000. Flack parameter x = 0.1(4) determined using 1433 selected quotients by Parsons method. The crystals were grown by slow evaporation of a methanol solution of (*S*)-**1** at r.t.

2.3.3. Crystallographic Data for *ras*-**1**

$C_{12}H_{19}NO_3$, colorless prism (0.164 × 0.162 × 0.140 mm^3), formula weight 225.28 g mol^{-1}; tetragonal, $P\bar{4}2_1c$ (No. 114), a = 14.9145(5) Å, c = 11.3489(6) Å, V = 2524.5(2) Å^3, Z = 8, Z' = 1, T = 105(2) K, d_{calc} = 1.185 g cm^{-3}, μ(Mo *Kα*) = 0.085 mm^{-1}, $F(000)$ = 976; $T_{max/min}$ = 0.9844/0.8807; 48277 reflections were collected ($1.931° \leq \theta \leq 25.726°$, index ranges: $-18 \leq h \leq 18$, $-18 \leq k \leq 18$, and $-13 \leq l \leq 13$), 2398 of which were unique, R_{int} = 0.0806, R_σ = 0.0265; completeness to θ of 25.726° 100.0%. The refinement of 159 parameters with 3 restraints converged to $R1$ = 0.0525 and $wR2$ = 0.1320 for 2119 reflections with $I > 2\sigma(I)$, $R1$ = 0.0601 and $wR2$ = 0.1376 for all data with goodness-of-fit S = 1.076 and residual electron density $\rho_{max/min}$ = 0.321 and −0.208 e Å^{-3}, rms 0.058; max shift/e.s.d. in the last cycle 0.000. Flack parameter x = −0.1(5) determined using 816 selected quotients by Parsons method. The crystals were grown by slow evaporation of a methanol solution of *rac*-**1** at r.t.

2.3.4. Crystallographic Data for (*R*)-**2**

$C_9H_{12}O_4$, colorless plank (0.260 × 0.199 × 0.069 mm^3), formula weight 184.19 g mol^{-1}; monoclinic, $P2_1$ (No. 4), a = 5.68626(12) Å, b = 7.26521(15) Å, c = 10.62856(19) Å, β = 90.8562(18)°, V = 439.037(15) $Å^3$, Z = 2, Z' = 1, T = 94(2) K, d_{calc} = 1.393 g cm^{-3}, μ(Mo $K\alpha$) = 0.110 mm^{-1}, F(000) = 196; $T_{max/min}$ = 1.000/0.503; 22777 reflections were collected (3.397° ≤ θ ≤ 33.436°, index ranges: −8 ≤ h ≤ 8, −11 ≤ k ≤ 11, and −16 ≤ l ≤ 16), 3254 of which were unique, R_{int} = 0.0309, R_σ = 0.0193; completeness to θ of 33.436° 96.7%. The refinement of 130 parameters with 4 restraints converged to $R1$ = 0.0339 and $wR2$ = 0.0930 for 3109 reflections with $I > 2\sigma(I)$, $R1$ = 0.0356 and $wR2$ = 0.0938 for all data with goodness-of-fit S = 1.074 and residual electron density; $\rho_{max/min}$ = 0.457 and −0.209 e $Å^{-3}$, rms 0.050; max shift/e.s.d. in the last cycle 0.000. Flack parameter x = −0.2(2) was determined using 1375 selected quotients by Parsons method. The crystals were grown by slow evaporation of an ethyl acetate solution of (*R*)-**2** at r.t. It should be noted that the crystals obtained from a racemic solution are characterized by the same unit cell constants and crude structure but significantly smaller crystal dimensions and consequently weaker diffraction ability.

3. Results and Discussion

3.1. Synthesis of (S)-Prenalterol

Prenalterol **1**, 1-(4-hydroxyphenoxy)-3-(isopropylamino)-2-propanol (Scheme 1), is a partial adrenergic agonist with functional β_1-receptor specificity [14–16]. It is effective in the treatment of acute cardiac failure, postmyocardial infarction low-output syndrome, shock, and is useful in the treatment of β-blocker overdosage [16,17].

The main source for obtaining enantiopure prenalterol is natural D-mannitol. There are many patents on which, with slight variations, the target product is obtained from this row material. All these schemes include many stages and cannot do without the introduction and removal of protective groups (isopropylidene, mesyl, tosyl, benzyl, etc.). One of the schemes (Scheme 2) is shown below [18].

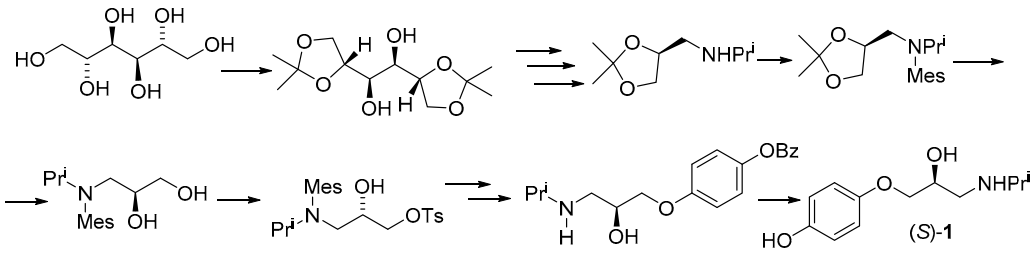

Scheme 2. Synthesis of prenalterol (*S*)-**1** from natural D-mannitol.

The main alternative to the use of natural compounds to obtain practically useful substances in an enantiopure form is still the resolution of synthetic racemic raw materials at one stage or another of obtaining the final product. Among the many ways of chiral resolution [19], we focused on direct approaches based on the spontaneous separation of enantiomers upon crystallization [20]. The history and current state of the subject, as well as examples of the application of this approach to the production of single-enantiomeric drugs, are reviewed in [21].

Active interest in the phenomenon of spontaneous resolution allowed us to discover this property in 3-(4-hydroxyphenoxy)propane-1,2-diol **2** (Scheme 1). In our preliminary report [11], we drew attention to the significant difference in the melting points of the *rac*-**2** and *scal*-**2** samples (127–129 °C and 150–151 °C, respectively), which suggested that the dependence of the melting of the samples of this diol on their enantiomeric composition was characterized by a phase diagram with a minimum for the racemate. This type of phase diagram allows the possibility of direct resolution of *rac*-**2** into individual enantiomers, which was implemented by us by the entrainment procedure. Our proposed approach to enantiopure (*S*)-**1** is shown in Scheme 3.

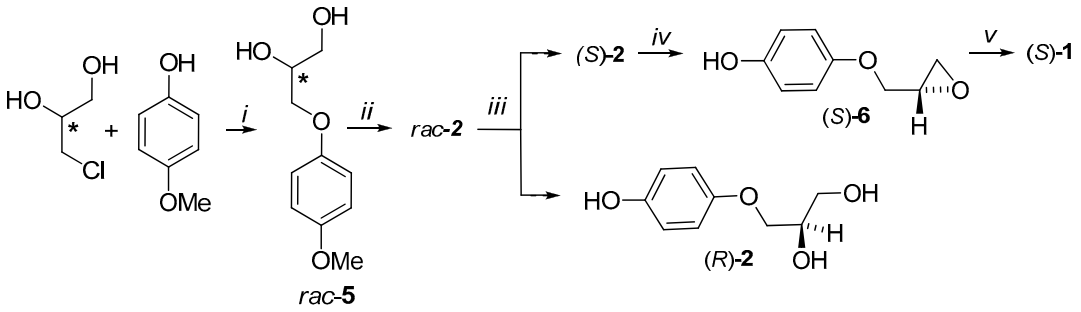

Scheme 3. Synthesis of (*S*)-**1** from racemic 3-(4-hydroxyphenoxy)propane-1,2-diol *rac*-**2**. Reagents and conditions: (i) NaOH, EtOH, and reflux; (ii) HBr (45% aq.), 50 °C; (iii) resolution by entrainment; (iv) PPh_3, DEAD, THF, and reflux; (v) *i*-$PrNH_2$ and reflux. Explanations are in the text. Asterisks in the diagram indicate chiral centers.

Commenting on this scheme, one should discuss the availability of diol **2**. Usually, for the synthesis of 3-aryloxypropane-1,2-diols, the interaction of 3-chloropropanediol with the corresponding phenol in the basic medium is used. However, in the case of pyrocatechol, the yield of the target product is low (about 25%) due to side oxidative processes. As was to be expected, in the case of hydroquinone, this factor is even more significant, and diol **2** can be obtained by this way with a yield of only approximately 10%. In order to avoid the side processes, we turned to the available *para*-methoxyphenol, in which one of the hydroxy groups of hydroquinone is formally protected. As a result of its reaction with chloropropanediol, *para*-methoxy-substituted diol **5** is obtained with a yield of 65%. Target diol *rac*-**2** was obtained by hydrolysis of diol **5** in the presence of HBr with 61% yield. Enantiopure 3-(4-hydroxyphenoxy)propane-1,2-diols **2** were obtained by chiral resolution of racemic diol **2** using the preferential crystallization approach, when the crystallization of an individual enantiomer is provoked by the introduction of an enantiopure crystal seed into a supersaturated racemic solution in water. In total, for three cycles (six runs) out of 5.3 g of *rac*-**2**, the yield of pure enantiomer (*S*)-**2** was about 1 g, and (*R*)-**2** 0.9 g [11].

Further, (*S*)-**2** was converted to 4-(2,3-epoxypropoxy)phenol (*S*)-**6** via the Mitsunobu reaction. (*S*)-prenalterol, (*S*)-**1** was obtained by the interaction of epoxide (*S*)-**6** with isopropylamine. The proposed scheme compares favorably with the known "chiral pool" approaches by a smaller number of stages and the use of racemic raw materials.

Finally, samples of *rac*-**1** and (*S*)-**1**, obtained according to Scheme 3, as well as a non-racemic sample of diol (*R*)-**2**, were examined by SC-XRD.

3.2. SC-XRD Results

3.2.1. 3-(4-Hydroxyphenoxy)propane-1,2-diol **2**

A randomly selected crystal from a racemic sample of diol **2** was solved in Sohncke group $P2_1$ (4), which reliably proves the spontaneous resolution of this diol during crystallization. For further analysis, we used good crystals of the single-enantiomeric sample of diol (*R*)-**2**, the data of the X-ray diffraction experiment for which are given in Section 2.3.4. The structure of the molecule in crystals and the subsequent numbering of potential donors and acceptors of intermolecular hydrogen bonds (IMHB) are given in Figure 1a.

The search in the Cambridge Structural Database (CSD version 5.42 of September 2021, ConQuest version 2021.2.0) found 60 refcodes belonging to structures with the general formula R−$OCH_2CH(OH)CH_2OH$, where R is an aromatic or heterocyclic fragment. It turned out that the data for 54 of them, corresponding to 33 compounds with different connectivity formulas, were obtained in our research group.

A specific feature of this family is its unusually high frequency of manifesting the property of spontaneous resolution, which was revealed for 17 (>50%) of the studied structures. This feature has been previously exploited for the synthesis of single-enantiomeric drugs xibenolol [22], mexiletine [23], pindolol [24], and some new bioactive aminopropanols

under development [25]. Other examples of the use of direct racemate resolution methods for the preparation of enantiopure drugs from our and world practice are collected in an already cited review [21].

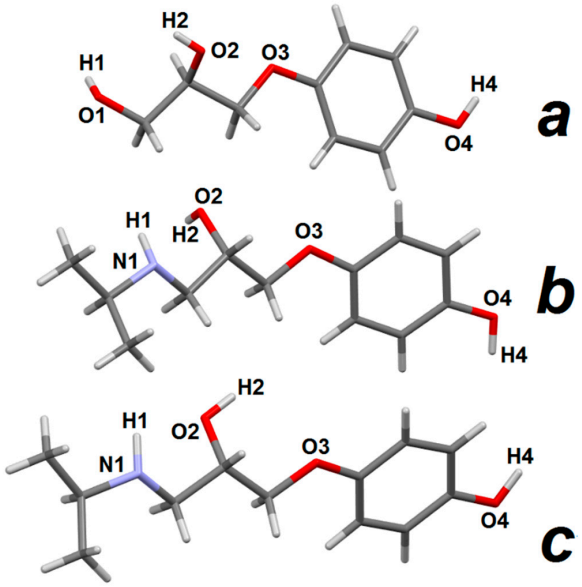

Figure 1. Accepted partial numbering of atoms and structure of molecules in: (**a**) (*R*)-**2;** (**b**) (*S*)-**1** crystals; and (**c**) (*S*)-**1** molecules in *rac*-**1** crystals.

As it was stated in the informative review [26] "the understanding and prediction of spontaneous resolution . . . remains one of the true challenges for science in the 21st century". Accurate knowledge of the crystal structure of a substance exhibiting such a property may be a small but useful contribution to the solution of this problem.

The main supramolecular motif in diol **2** crystals is chains, the elementary link of which (Figure 2) is formed with the participation of three molecules held together by three different intermolecular hydrogen bonds (IMHB). The primary hydroxyl of the conditionally first molecule forms IMHB O1−H1···O2 with the oxygen atom of the secondary hydroxyl of the second molecule. Further, the hydrogen atom of this group forms IMHB O2−H2···O4 with the oxygen atom of the phenolic group of the third molecule, and the hydrogen bond O4−H4···O1′ completes the link of the infinite chain, which, in terms of Etter−Bernstein [27,28], is denoted as $\mathbf{C_3^3(6)}$.

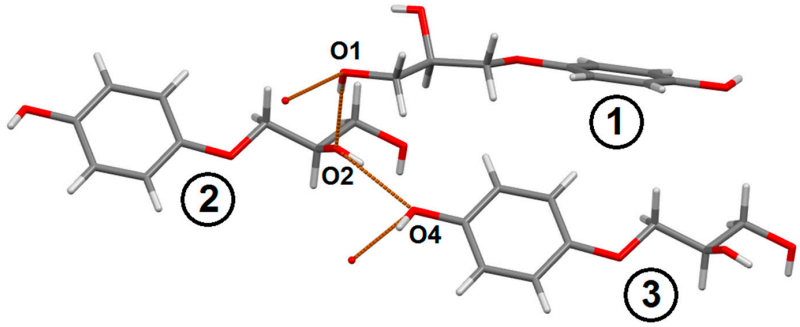

Figure 2. Elementary link of the $\mathbf{C_3^3(6)}$ chain in (*R*)-**2** diol crystals. The numbers 1–3 in circles represent the molecules discussed in the text.

In the crystal, these $\mathbf{C_3^3(6)}$ chains form around helical axes 2_1 parallel to the 0*b* direction, forming endless spirals, right-handed *P* in the case of *R*-enantiomers, and left-handed *M* in the case of *S*-enantiomers (Figure 3). As a result, each of the diol molecules simultaneously participates in three parallel chains, thus, generating a monolithic 3D crystal structure with a high (71.2%) value of packing index.

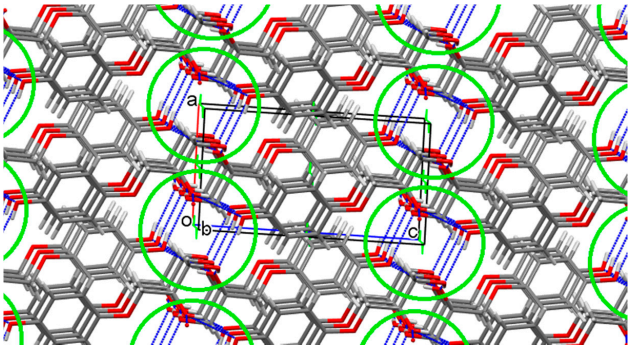

Figure 3. Packing of molecules in crystals of diol (*R*)-**2**. Helical chains $\mathbf{C_3^3(6)}$ forming around the 2_1 axes are marked with green circles.

A comparison of the packings of all aromatic ethers of glycerol prone to spontaneous resolution is beyond the scope of this work. We only note that the case of diol **2** is distinguished by the fact that not only the hydroxyl groups of the glycerol fragment, as was the case in all previously studied examples, but also the hydroxyl of the aromatic substituent are involved in the formation of the main supramolecular motif.

3.2.2. Prenalterol **1**

Non-racemic prenalterol crystallizes in the Sohncke group $P2_12_12_1$ (19) with a single molecule in the asymmetric cell. Figure 4a illustrates the realization in crystals of enantiopure prenalterol (*S*)-**1** of the $\mathbf{C_1^1(5)}$ chain, the connecting element of which (except for the body of molecules) is the only IMHB O2−H2···N1. Note that in (*S*)-**1** crystals, the donor hydrogen atom of the amino group H1 and the acceptor atom O3 (see Figure 1) are sterically shielded and do not participate in intermolecular hydrogen bonds. Chain $\mathbf{C_1^1(5)}$ is folded around a helical axis 2_1 parallel to direction 0*a*. Figure 4b, in which the atoms participating in the chain are highlighted using spacefill style, clearly shows the helical *M*-character of this chain.

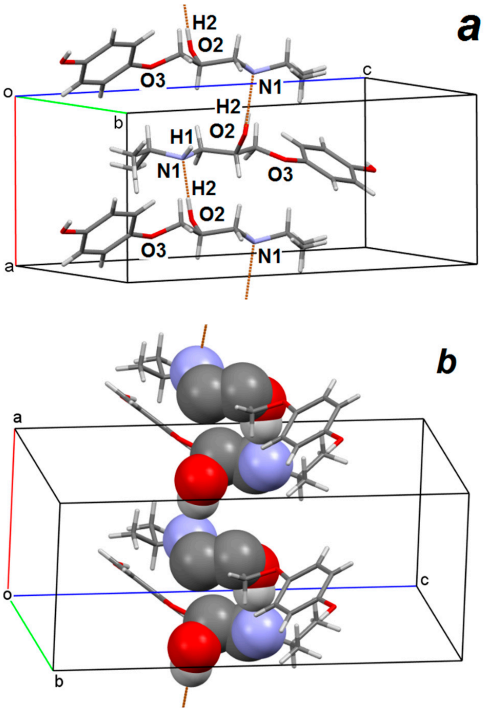

Figure 4. Chain $\mathbf{C_1^1(5)}$ in crystals of prenalterol (*S*)-**1**: (**a**) Illustrates the details of chain formation; (**b**) emphasizes its helical nature.

It follows from Figure 4 that the hydroxyl groups of the phenolic fragments of prenalterol do not take part in the formation of linear (chain) supramolecular motifs. However, due to IMHB O4–H4···O2, the spiral columns are combined into a single bilayer parallel to the 0*ab* plane (Figure 5). The bilayers, limited along the periphery by hydrophobic isopropyl groups and lateral fragments of benzene rings, form a single crystalline packing due to hydrophobic interactions with a packing index of 67.9%.

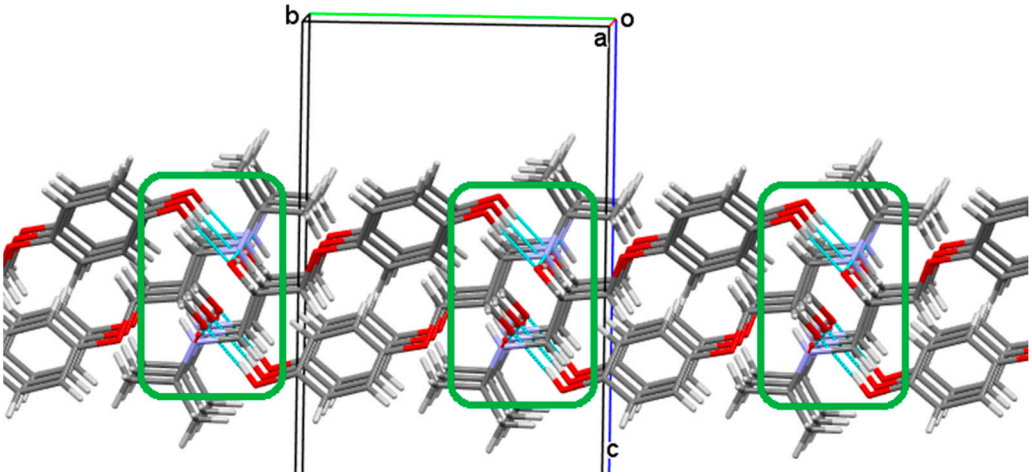

Figure 5. A bilayer formed in (*S*)-**1** crystals by combining $\mathbf{C_1^1(5)}$ chains, highlighted in green frames, due to intermolecular hydrogen bonds O4–H4···O2 with the participation of hydroxyl groups of phenol fragments unoccupied in the formation of chains.

Racemic prenalterol crystallizes in the non-centrosymmetric tetragonal space group $P\bar{4}2_1c$ (114) with a single molecule in the asymmetric cell. The systems of intermolecular hydrogen bonds in the crystals of racemic and enantiopure prenalterol largely coincide, but differences in the symmetry of the space groups lead to different crystal-forming associates. If the O2−H2···N1 IMHB sequence, organized around the helical axis 2_1 in (*S*)-**1** crystals, generates a 1D chain $\mathbf{C_1^1(5)}$ (Figure 4), then, the same sequence in *rac*-**1** crystals organized around the rotoinversion axis $\bar{4}$ closes in 0D ring $\mathbf{R_4^4(20)}$ (Figure 6).

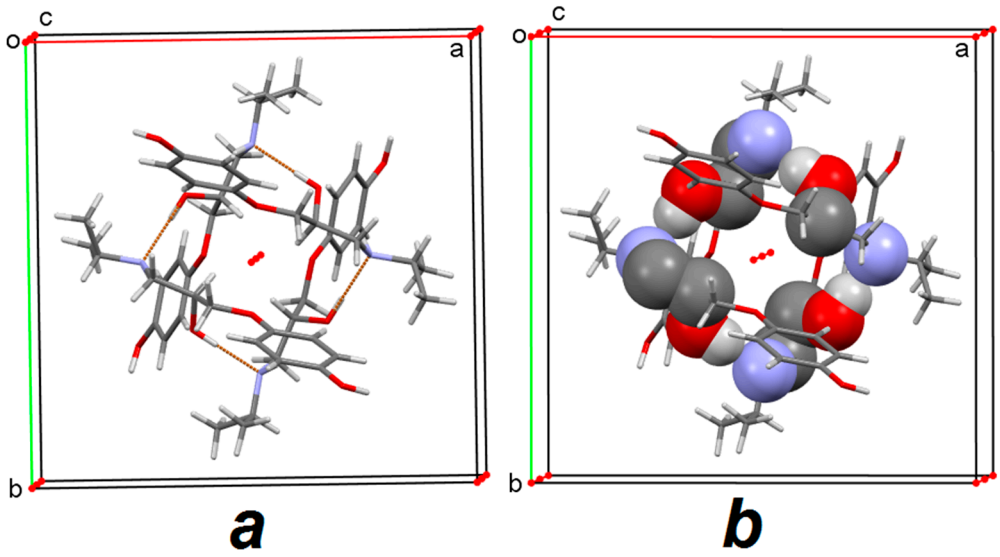

Figure 6. $\mathbf{R_4^4(20)}$ ring in prenalterol *rac*-**1** crystals: (**a**) illustrates the details of IMBH formation; (**b**) emphasizes its ring nature.

Similar to the case of (*S*)-**1**, the hydrogen atom of the amino group H1 and the atom O3 (see Figure 1) do not participate in intermolecular hydrogen bonds, and the hydroxyl group of the phenolic fragment, due to the formation of IMHB O4–H4···O2, binds primary rings $\mathbf{R_4^4(20)}$ to each other. However, since the O4–H4···O2 hydrogen bonds are oriented along all three crystallographic directions, the resulting IMHB network generates a 3D monolith with a packing index of 66.0%.

A comparison of only two crystal packings is an unreliable basis for generalizations. We attempted to expand the core set with structures deposited in CSD, where we found three such pairs, namely (*S*)-atenolol and *rac*-atenolol (refcodes CIDHAZ and CEZVIN), (*S*)-propranolol and *rac*-propranolol (refcodes IMITON and PROPRA10), (*S*)-pindolol and *rac*-pindolol (refcodes XALYIV and PINDOL, PINDOL01). Unfortunately, the quality of the crystallographic data for the first pair did not allow them to be used for comparison. The other two pairs are compared below.

3.2.3. Propranolol **3**

Non-racemic (*S*)-**3**, (*S*)-1-(isopropylamino)-3-(1-naphthyloxy)propan-2-ol (Scheme 1) was studied by SC-XRD earlier (refcode IMITON) [29]. The structure of its molecule and the accepted partial numbering of atoms is shown in Figure 7a. The structure of the *S*-molecule of propranolol in *rac*-**3** crystals (Figure 7b) is given according to the literature data (refcode PROPRA10 [30]).

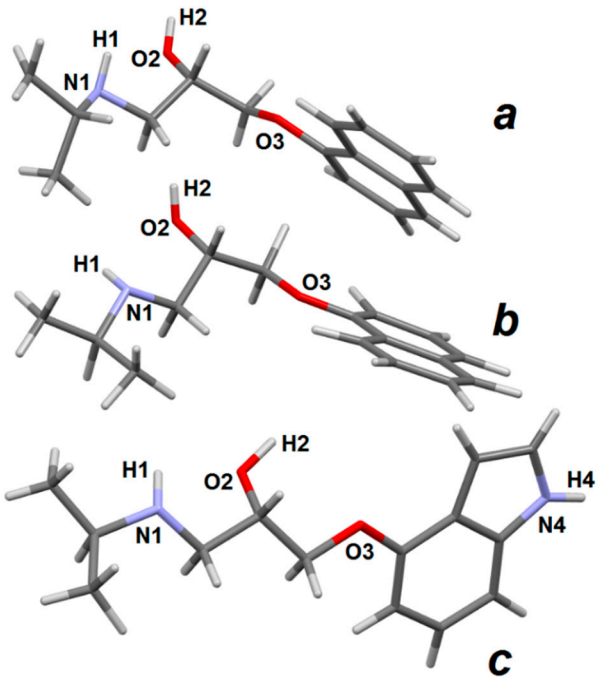

Figure 7. Accepted partial atomic numbering and molecular structure in: (**a**) non-racemic propranolol (*S*)-**3** crystals; (**b**) (*S*)-propranolol molecule in *rac*-**3** crystals; (**c**) (*S*)-pindolol molecule in *rac*-**4** crystals.

The single-enantiomeric (*S*)-**3** crystallizes in the Sohncke $P2_1$ (4) group. Similar to the case of enantiopure prenalterol (*S*)-**1**, the main and only structure formatting element in its crystals is the endless chain $\mathbf{C_1^1(5)}$, formed due to the intermolecular H-bond O2–H2···N1 around the helical axis 2_1, parallel to the direction 0*b* (Figure 8). The only, and in this case insignificant, difference is that the helices that arise in (*S*)-**3** crystals have a right-handed *P* character.

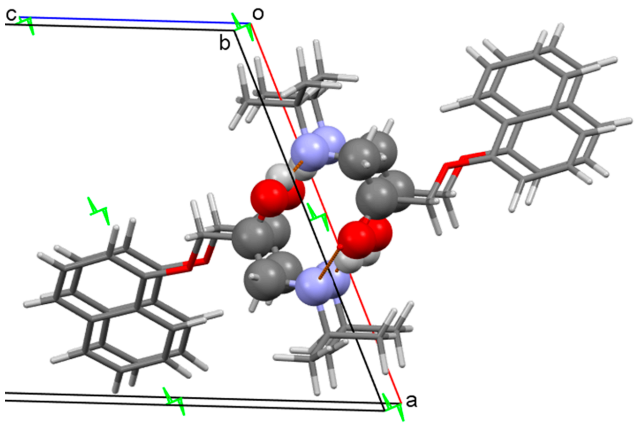

Figure 8. $\mathbf{C_1^1(5)}$ (*P* helix) chain formed around helical axis 2_1 in crystals of non-racemic propranolol (*S*)-**3**.

In (*S*)-**3** crystals, each sequence is an infinite relatively isolated 1D cylinder "bristled" with hydrophobic naphthyl and isopropyl fragments. Each cylinder is surrounded by six similar cylinders, and thus, the final 3D structure of the crystal is formed.

Racemic propranolol *rac*-**3** crystallizes in the centrosymmetric group $P2_1/c$ (**14**). In this case, the main supramolecular motif turns out to be 0D ring $\mathbf{R_2^2(10)}$ held together by a pair of the same IMHB O2–H2···N1 (Figure 9).

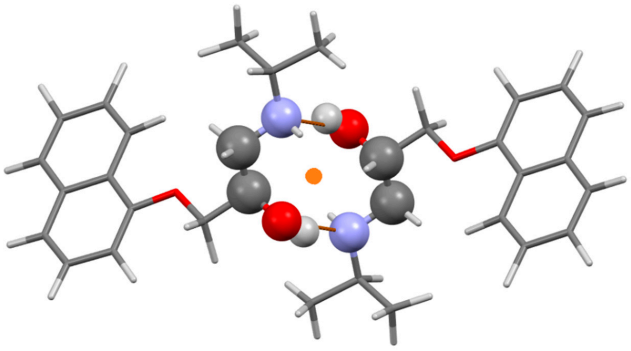

Figure 9. $\mathbf{R_2^2(10)}$ ring formed around the inversion center in *rac*-**3** crystals.

Approaching along the 0*b* direction, the rings form 1D columns (Figure 10), very similar to the hydrogen-bonded columns in (*S*)-**3** crystals (Figure 8). Not surprisingly, when forming the final 3D packing, each pseudo-column is surrounded by six similar ones.

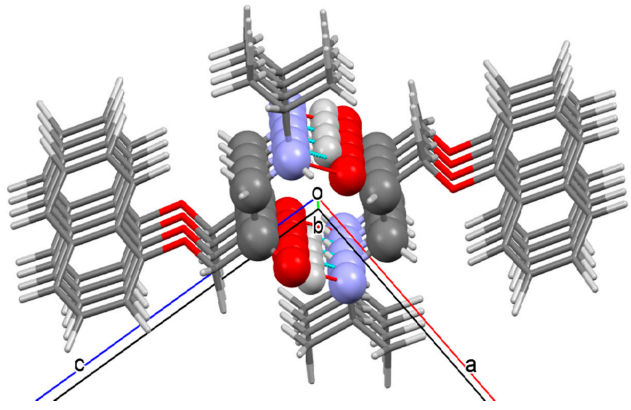

Figure 10. 1D column formed by $\mathbf{R_2^2(10)}$ rings along the *0b* direction in *rac*-**3** crystals.

3.2.4. Pindolol **4**

Racemic pindolol, 4-(2-hydroxy-3-isopropylamino-propoxy)-indole (Scheme 1), was examined twice by SC-XRD in [31] (PINDOL) and [32] (PINDOL01). The main results obtained in both papers practically coincide, but only the cif-file from [31], which we use below, allows us to correctly reproduce the packing details. The structure of pindolol and the partial atomic numbering adopted below in the fragments of interest to us are shown in Figure 7c.

Already a visual comparison of Figures 1c and 7c demonstrates a significant affinity of pindolol and prenalterol molecules in racemic crystals in terms of physical size, the number of fragments potentially capable of intermolecular hydrogen bonding, their relative arrangement, and orientation. The difference between these molecules is that the hydroxyl group of the phenolic fragment O4–H4 in the *rac*-**1** molecule corresponds to the N4–H4 group in the *rac*-**4** molecule. However, it can be expected that both of these fragments will behave in a similar way in the role of the IMHB link.

The compounds both crystallize in the same $P\bar{4}2_1c$ space group. According to CCDC information dated 1 January 2022 [33] from 1,171,413 structures for which the space group is fully defined, only 1355 structures, i.e., 0.001%, adopt this group. The relatively low population of one group or another is undoubtedly associated with strict and specific requirements for the structure of a molecule during its packing in a crystal. Taking into account the circumstances just listed, it was not surprising to find that the crystal organization of *rac*-**4** (Figure 11) repeats in detail that of *rac*-**1** (Figure 6).

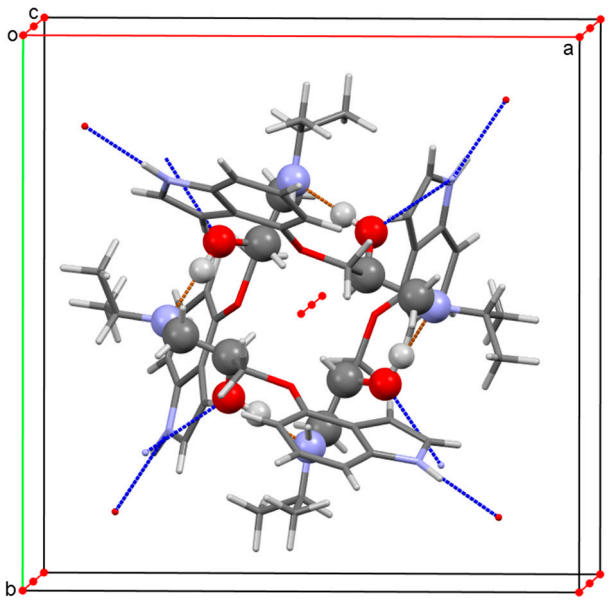

Figure 11. $R_4^4(20)$ ring in racemic pindolol crystals. Atoms are marked with ball-and-stick style, and intermolecular hydrogen bonds O2–H2···N1, forming a ring, are marked with a red dotted line. The blue dotted line marks N4–H4···O2 IMHB that bind rings to each other.

About thirty years ago, it was noticed that the ratios of macroscopic characteristics of racemic and enantiopure crystalline samples, such as melting points (T_f) and enthalpies of fusion (ΔH_f), for pindolol **4** fell out of the general range for β-adrenergic receptor antagonists. For example, for *rac*-**3**, T_f = 92.9° and ΔH_f = 38.1 kJ·mol^{-1}, and for (*S*)-**3** the same values are 71.4° and 34.2 kJ·mol^{-1}, i.e., they turn out to be relatively close. At the same time, for *rac*-**4**, T_f = 169.7 ° and ΔH_f = 57.9 kJ·mol^{-1}, and for (*S*)-**4** the same values are 92.0° and 25.7 kJ mol^{-1}, that is, they differ very noticeably [34]. Later, having studied the crystal structure of (*S*)-**4**, we connected this anomaly with the anomalous crystal structure of the latter, namely, with the presence of six (!) symmetry independent molecules in its unit

cell. This in turn led to a very loose structure, packing index of which (66.0%) approached the lower limit of existence of crystalline matter (approximagtely 60%) [24].

The system of intermolecular hydrogen bonds in crystals with a large number of independent molecules (Figure 12) cannot be organized around some obvious symmetry element, and for this reason it is difficult to analyze it in the usual terms.

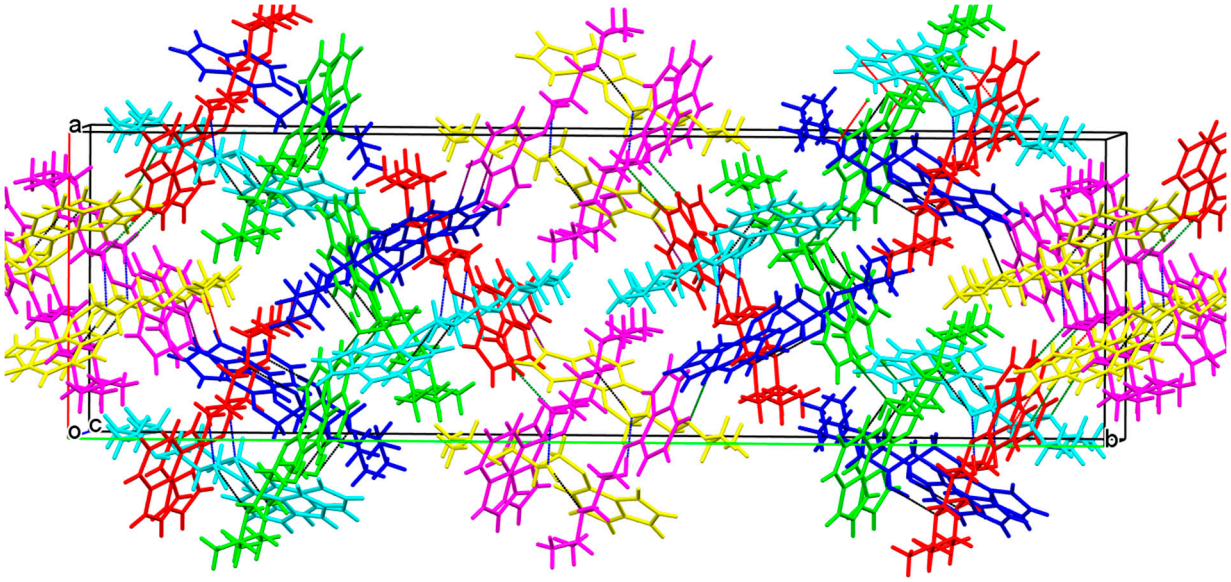

Figure 12. Intermolecular hydrogen bonds in (*S*)-pindolol (*S*)-**4** crystals. Six symmetrically independent molecules are marked with different colors.

Instead, we tried to estimate the frequency of occurrence of certain types of IMHB in (*S*)-**4** crystals. In this case, as an analyzed sample, molecules were used, which wholly or at least by a fragment, fell within the limits of significance in terms of its volume unit cell. In this array, we recorded 24 cases (44%) of the implementation of IMHB O2–H2···N1 (indicated by the black dotted line in Figure 12), 16 cases (30%) of O2–H2···O2 (blue dotted line), 10 cases (19%) of IMHB N4–H4···O2 (green dotted line), and 4 cases (7%) of N4–H4···N1 hydrogen bond (purple). Being aware of the limited rigor of such an analysis, we nevertheless note that the etheric oxygen atom O3 as an acceptor and the H1 atom as a IMHB donor, as in the previously studied cases, did not take part in hydrogen bonds, but IMHB O2–H2···N1 and O2–H2···O2 again turned out to be the main elements of the crystal packing.

4. Conclusions

A rare and specific property of 3-(4-hydroxyphenoxy)propane-1,2-diol **2**, which acts as a key reagent in the new synthesis of the enantiopure partial adrenergic agonist prenalterol **1**, is its ability to spontaneously resolve into enantiomers during crystallization. Diol **2** belongs to the family of terminal aromatic ethers of glycerol, while its crystal structure differs markedly from other members of the family prone to spontaneous resolution. The three diol molecules, each of which provides a different hydroxyl group than the other two members, take part in the formation of the elementary link of the $\mathbf{C_3^3(6)}$ helical chains that form the compound **2** crystal packing (Figure 2). Thus, both the hydroxyl groups of the glycerol fragment and the hydroxyl of the aromatic substituent take part in the formation of the main supramolecular motif (SMM).

Regardless of the structure of prenalterol **1**, propranolol **3,** and pindolol **4** studied in this work, their enantiomeric composition (racemic or single-enantiomeric form) and the symmetry of the crystal lattices, the donor hydrogen atom H1 of the amino group N1–H1, and the acceptor oxygen atom O3 do not take part in the formation of supramolecular

motifs in their crystals. In this case, the main SMM in all the studied crystals is formed due to the IMHB O2–H2···N1.

At the same time, the nature of the main supramolecular motifs realized in crystals of the same adrenoactive drugs turns out to be pronouncedly chiral dependent. While infinite $\mathbf{C_1^1(5)}$ chains are realized in single-enantiomeric crystals **1** and **3**, closed cyclic structures arise in racemic crystals, $\mathbf{R_4^4(20)}$ in cases **1** and **4**, and $\mathbf{R_2^2(10)}$ in case **3**. This regularity, chain vs. ring, we have already noted in the study of chiral 1,3-oxazolidin-2-ones [35] and alkyl-substituted aromatic esters of glycerol [36]. In the latter case, the change in the nature of SMM was accompanied by a striking change in macroscopic characteristics, i.e., while non-racemic samples turned out to be effective low-molecular-weight gelators, racemates were completely devoid of such ability.

The results obtained again demonstrate the influence of the chiral polarization of a substance not only on the general (selection of a space group) but also on particular characteristics of matter crystal organization, for example, selection of a specific SMM.

Author Contributions: Conceptualization, writing—original draft preparation, writing—review and editing, A.A.B.; SC-XRD experiments, R.R.F.; methodology, samples preparation, proofread the manuscript, Z.A.B. All authors have read and agreed to the published version of the manuscript.

Funding: This research received no external funding.

Institutional Review Board Statement: Not applicable.

Informed Consent Statement: Not applicable.

Data Availability Statement: Not applicable.

Acknowledgments: X-ray diffraction data were registered on the equipment of the Assigned Spectral-Analytical Center of the FRC Kazan Scientific Center of RAS. The authors thank A.V. Kurenkov for valuable technical assistance.

Conflicts of Interest: The authors declare no conflict of interest.

References

1. Kant, I. *Prolegomena to Any Future Metaphysics that Will be Able to Come Forward as Science*; Cambridge University Press: Cambridge, UK, 2004.
2. Kelvin, W.T. Molecular tactics of a crystal. *J. Oxf. Univ. Jr. Sci. Club* **1894**, *18*, 25, (DLC) 12034810.
3. Gal, J.; Cintas, P. Early history of the recognition of molecular biochirality. *Top. Curr. Chem.* **2012**, *333*, 1–40. [CrossRef]
4. Gal, J. Molecular chirality in chemistry and biology: Historical milestones. *Helv. Chim. Acta* **2013**, *96*, 1617–1657. [CrossRef]
5. Wagniére, G.H. *On Chirality and the Universal Asymmetry: Reflections on Image and Mirror Image*; Wiley-VCH: Zürich, Switzerland, 2007; ISBN 978-3-906-39038-3.
6. Devínsky, F. Chirality and the origin of life. *Symmetry* **2021**, *13*, 2277. [CrossRef]
7. U.S. Food and Drug Administration. Guidance Document, Development of New Stereoisomeric Drugs. May 1992. Available online: https://www.fda.gov/regulatory-information/search-fda-guidance-documents/development-new-stereoisomeric-drugs (accessed on 15 May 2022).
8. Brooks, W.H.; Guida, W.C.; Daniel, K.G. The significance of chirality in drug design and development. *Curr. Top. Med. Chem.* **2011**, *11*, 760–770. [CrossRef]
9. Mullin, R. Tufts study finds big rise in cost of drug development. *Chem. Eng. News* **2014**, *92*, Iss.47. Available online: https://cen.acs.org/articles/92/web/2014/11/Tufts-Study-Finds-Big-Rise.html (accessed on 15 May 2022).
10. *The Merck Index*, 14th ed.; O'Neil, M.J. (Ed.) Merck and Co.: Whitehouse Station, NJ, USA, 2006; p. 1329, Entry 7735.
11. Bredikhina, Z.A.; Kurenkov, A.V.; Bredikhin, A.A. Effective synthesis of non-racemic prenalterol based on spontaneous resolution of 3-(4-hydroxyphenoxy)propane-1,2-diol. *Mendeleev Commun.* **2019**, *29*, 198–199. [CrossRef]
12. Sheldrick, G.M. SHELXT—Integrated space-group and crystal-structure determination. *Acta Crystallogr. Sect. A Found. Adv.* **2015**, *71*, 3–8. [CrossRef]
13. Sheldrick, G.M. Crystal structure refinement with SHELXL. *Acta Crystallogr. Sect. C Struct. Chem.* **2015**, *71*, 3–8. [CrossRef]
14. Kenakin, T.P.; Beek, D. Is Prenalterol (H133/80) really a selective beta1 adrenoceptor agonist? *Tissue selectivity resulting from differences in stimulus-response relationships. J. Pharmacol. Exp. Ther.* **1980**, *213*, 406–412.
15. Mattsson, H.; Andersson, T.; Carlsson, E.; Hedberg, A.; Lundgren, B.; Olsson, T. Beta 1-and beta 2-adrenoceptor stimulatory effects of prenalterol. *Naunyn Schmiedebergs Arch. Pharmacol.* **1982**, *321*, 302–308. [CrossRef]

16. Waller, D.G. Beta-adrenoceptor partial agonists: A renaissance in cardiovascular therapy? *Br. J. Clin. Pharmacol.* **1990**, *30*, 157–171. [CrossRef] [PubMed]
17. Barisione, G.; Baroffio, M.; Crimi, E.; Brusasco, V. Beta-adrenergic agonists. *Pharmaceuticals* **2010**, *3*, 1016–1044. [CrossRef] [PubMed]
18. Fahrenholtz, K.E.; Guthrie, R.W.; Kierstead, R.W.; Tilley, J.W. Piperazine derivatives. Patent DE 2904799, 9 August 1979.
19. Lorenz, H.; Seidel-Morgenstern, A. Processes to separate enantiomers. *Angew. Chem. Int. Ed.* **2014**, *53*, 1218–1250. [CrossRef] [PubMed]
20. Amabilino, D.B.; Kellogg, R.M. Spontaneous deracemization. *Isr. J. Chem.* **2011**, *51*, 1034–1040. [CrossRef]
21. Bredikhin, A.A.; Bredikhina, Z.A. Stereoselective crystallization as a basis for single-enantiomer drug production. *Chem. Eng. Technol.* **2017**, *40*, 1211–1220. [CrossRef]
22. Bredikhin, A.A.; Bredikhina, Z.A.; Kurenkov, A.V.; Gubaidullin, A.T. Synthesis, crystal structure, and absolute configuration of the enantiomers of chiral drug xibenolol hydrochloride. *Tetrahedron Asymmetry* **2017**, *28*, 1359–1366. [CrossRef]
23. Bredikhina, Z.A.; Kurenkov, A.V.; Krivolapov, D.B.; Bredikhin, A.A. Stereoselective crystallization of 3-(2,6-dimethylphenoxy)propane-1,2-diol; preparation of the single-enantiomer drug mexiletine. *Tetrahedron Asymmetry* **2015**, *26*, 577–583. [CrossRef]
24. Bredikhin, A.A.; Bredikhina, Z.A.; Kurenkov, A.V.; Krivolapov, D.B. Synthesis and crystal structure of (S)-pindolol. *Tetrahedron Asymmetry* **2017**, *28*, 442–446. [CrossRef]
25. Bredikhin, A.A.; Zakharychev, D.V.; Bredikhina, Z.A.; Kurenkov, A.V.; Samigullina, A.I.; Gubaidullin, A.T. Stereoselective crystallization of chiral 3,4-dimethylphenyl glycerol ether complicated by plurality of crystalline modifications. *Crystals* **2020**, *10*, 201. [CrossRef]
26. Perez-Garcia, L.; Amabilino, D.B. Spontaneous resolution, whence and whither: From enantiomorphic solids to chiral liquid crystals, monolayers and macro- and supra-molecular polymers and assemblies. *Chem. Soc. Rev.* **2007**, *36*, 941–967. [CrossRef]
27. Etter, M.C. Encoding and decoding hydrogen-bond patterns of organic-compounds. *Acc. Chem. Res.* **1990**, *23*, 120–126. [CrossRef]
28. Bernstein, J.; Davis, R.E.; Shimoni, L.; Chang, N.L. Patterns in hydrogen bonding—functionality and graph set analysis in crystals. *Angew. Chem. Int. Ed.* **1995**, *34*, 1555–1573. [CrossRef]
29. Bredikhin, A.A.; Savel'ev, D.V.; Bredikhina, Z.A.; Gubaidullin, A.T.; Litvinov, I.A. Crystallization of chiral compounds. 2. Propranolol: Free base and hydrochloride. *Russ. Chem. Bull.* **2003**, *52*, 853–861. [CrossRef]
30. Ammon, H.L.; Howe, D.-B.; Erhardt, W.D.; Balsamo, A.; Macchia, B.; Macchia, F.; Keefe, W.E. The crystal structures of dichloroisoproterenol, propranolol and propranolol hydrochloride. *Acta Crystallogr. Sect. B Struct. Crystallogr. Cryst. Chem.* **1977**, *33*, 21–29. [CrossRef]
31. Gadret, M.; Goursolle, M.; Leger, J.M.; Colleter, J.C. Crystal-structure of Pindolol, 4-(2-hydroxy-3-isopropylaminopropoxy)indole. *Acta Crystallogr. Sect. B Struct. Crystallogr. Cryst. Chem.* **1976**, *32*, 17–20. [CrossRef]
32. Chattopadhyay, T.K.; Palmer, R.A.; Mahadevan, D. Molecular and absolute crystal structure-of Pindolol-1-(1H-indol-4-yloxy)-3-[(1-methylethyl)amino]-2-propanol—A specific beta-adrenoceptor antagonist with partial agonist activity. *J. Chem. Cryst.* **1995**, *25*, 195–199. [CrossRef]
33. The Cambridge Crystallographic Data Centre (CCDC). Available online: https://www.ccdc.cam.ac.uk/support-and-resoureces/ccdcresouces (accessed on 15 May 2022).
34. Neau, S.H.; Shinwari, M.K.; Hellmuth, E.W. Melting-point phase-diagrams of free-base and hydrochloride salts of Bevantolol, Pindolol and Propranolol. *Int. J. Pharm.* **1993**, *99*, 303–310. [CrossRef]
35. Bredikhin, A.A.; Bredikhina, Z.A.; Gubaidullin, A.T. Chirality-dependent supramolecular synthons based on the 1,3-oxazolidin-2-one framework: Chiral drugs mephenoxalone, metaxalone and 114 other examples. *CrystEngComm* **2020**, *22*, 7252–7261. [CrossRef]
36. Bredikhin, A.A.; Gubaidullin, A.T.; Bredikhina, Z.A.; Fayzullin, R.R.; Lodochnikova, O.A. Chirality, gelation ability and crystal structure: Together or apart? *Alkyl phenyl ethers of glycerol as simple LMWGs. Symmetry* **2021**, *13*, 732. [CrossRef]